Ocean Sci., 16, 1247–1259, 2020
https://doi.org/10.5194/os-16-1247-2020

Ocean Science Open Access EGU

Changes in detrital sediment supply to the central Yellow Sea since the last deglaciation

Hyo Jin Koo and Hyen Goo Cho

Department of Geology and Research Institute of Natural Science, Gyeongsang National University, Jinju 52828, Republic of Korea

Correspondence: Hyen Goo Cho (hgcho@gnu.ac.kr)

Received: 10 June 2020 – Discussion started: 26 June 2020
Revised: 22 August 2020 – Accepted: 1 September 2020 – Published: 27 October 2020

Abstract. The sediment supply to the central Yellow Sea since the last deglaciation was uncovered through clay mineralogy and geochemical analysis of core 11YS-PCL14 in the Central Yellow Sea Mud (CYSM). The core can be divided into four units based on the various proxies, such as grain size, clay mineralogy, geochemistry, and Sr and Nd isotopes: Unit 4 (700–520 cm; 15.5–14.8 ka), Unit 3 (520–310 cm; 14.8–12.8 ka), Unit 2 (310–130 cm; 12.8–8.8 ka), and Unit 1 (130–0 cm; < 8.8 ka). Unit 2 is subdivided into two subunits, Unit 2-2 (310–210 cm; 12.8–10.5 ka) and Unit 2-1 (210–130 cm; 10.5–8.8 ka), according to smectite content. Comparison of the clay mineral compositions, rare earth elements, and εNd indicate distinct provenance shifts in core 11YS-PCL14. Moreover, the integration of clay mineralogical and geochemical indices show different origins according to particle size. During the late last deglaciation (Units 3 and 4, 15.5–12.8 ka), Unit 4 sediments originated from all potential provenance rivers, such as the Huanghe, Changjiang, and western Korean rivers, while the source of coarse sediments changed to the Huanghe beginning with Unit 3. Fine-grained sediment was still supplied from all rivers during the deposition of Unit 3. Early Holocene (Unit 2) sediments were characterized by oscillating grain size, clay minerals, and moderate εNd values. In this period, the dominant fine-sediment provenance changed from the Huanghe to the Changjiang, whereas coarse sediments most likely originated from western Korean rivers. The Unit 1 CYSM sediments were sourced primarily from the Changjiang, along with minor contributions from the western Korean rivers. Possible transport mechanisms concerning such changes in the sediment provenance include paleo-river pathways, tidal stress evolution, and the development of the Yellow Sea Warm Current and coastal circulation systems, depending on the sea level fluctuations.

1 Introduction

The Yellow Sea, located between the China and Korean Peninsula, is a semi-enclosed epicontinental shelf with a complex oceanic circulation system (Fig. 1). It is notable for its large amount of runoff and terrigenous sediment supplied from several adjacent rivers, including two of the world's largest rivers, the Changjiang and Huanghe, as well as from several smaller Korean rivers, including the Han, Keum, and Yeongsan rivers. Although most riverine sediments are trapped in estuaries and along coastal areas, some are deposited on adjacent shelves (Milliman et al., 1985, 1987), forming several shelf mud patch depositions such as Central Yellow Sea Mud (CYSM), Southeastern Yellow Sea Mud, and Southwestern Jeju Island Mud (Fig. 1). These deposits provide abundant information on paleo-environmental changes, sediment supply, marine hydrodynamics, and climate variation (e.g., Wang et al., 1999; Kim and Kucera, 2000; Li et al., 2014a; Cho et al., 2015; Kwak et al., 2016; Hu et al., 2018).

The provenance of CYSM sediments have attracted many researchers over the last 3 decades. Many studies have indicated that CYSM sediments originated mostly from the Huanghe, considering the large amount of sediment load carried by that river (Milliman et al., 1987; Lee and Chough, 1989; Liu et al., 2002; Yang and Liu, 2007; Shinn et al., 2007; Xiang et al., 2008). On the other hand, other studies have used mineralogical, geochemical, and magnetic observations

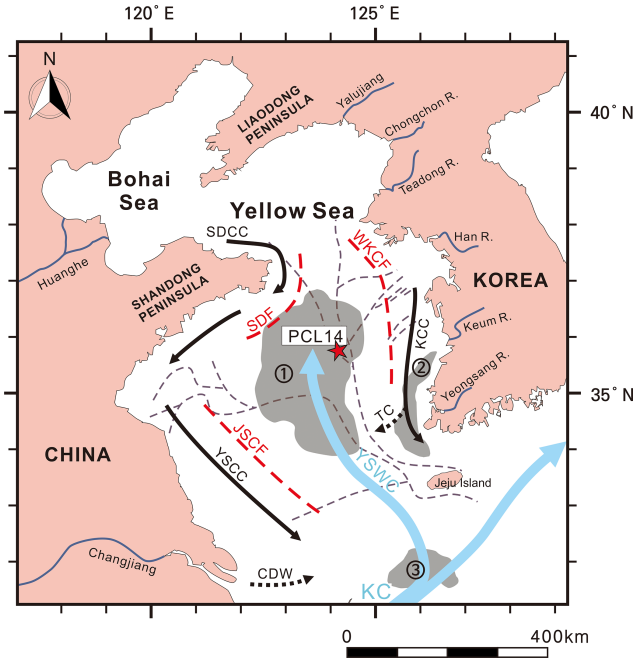

Figure 1. Schematic map showing the location of core 11YS-PCL14 and the surface circulation in the Yellow Sea (modified from Li et al., 2014a; Wang et al., 2014). The dotted gray lines indicate the paleo-river pathways (Yoo et al., 2016). Acronyms are defined as follows: (1) Central Yellow Sea Mud (CYSM), (2) Southeastern Yellow Sea Mud (SEYSM), (3) Southwestern Jeju Island Mud (SWCIM), Kuroshio Current (KC), Yellow Sea Warm Current (YSWC), Shandong Coastal Current (SDCC), Yellow Sea Coastal Current (YSCC), Korean Coastal Current (KCC), Shandong Front (SDF), Jiangsu Coastal Front (JSCF), Western Korean Coastal Front (WKCF).

and determined that the CYSM was formed from a complex mixture of sediments from the Huanghe, as well as the Changjiang and several Korean rivers (Zhao et al., 1990; Wei et al., 2003; Zhang et al., 2008; Li et al., 2014a; Wang et al., 2014; Koo et al., 2018). In addition, recent studies using core sediments suggested that the provenance of CYSM changed mainly from Huanghe to Changjiang with a minor contribution from the Korean rivers during the Holocene (Lim et al., 2015; Hu et al., 2018). However, the timing of the CYSM formation and the deposition environment prior to the Holocene remains unclear.

Discrimination of sediment source and reconstruction of paleo-environmental changes can be undertaken based on grain size, clay mineralogy, and elemental signals. In particular, clay mineralogy and geochemistry have been utilized as a powerful tool to trace provenance of the terrigenous fraction of marine sediments in the Yellow Sea (Yang et al., 2002; Yang and Youn, 2007; Liu et al., 2007, 2010b; Dou et al., 2010; Hu et al., 2012; Wang and Yang, 2013; Li et al., 2014a; Koo et al., 2018). Several additional factors can also control sedimentary characteristics, including terrigenous inputs, sea level, and climate conditions (Wang et al., 1999; Duck et al., 2001; Hwang et al., 2014; Li et al., 2014a; Lim et al., 2015; Badejo et al., 2016; Hu et al., 2018). In addition, paleo-river pathways, recently reconstructed by high-resolution seismic research in the Yellow Sea, can account for sedimentation and sediment provenance since the last deglaciation because they are an important route of sediment transport during the low stand period (KIGAM, 1993; Xu et al., 1997; Yoo et al., 2015, 2016).

In this study, we aim to determine the sediment provenance and transport mechanism of CYSM using clay mineralogy and geochemistry multi-proxy. The purposes are to provide a broad insight into the supply of CYSM sediments and to reconstruct the paleo-environment since the Last Glacial Maximum (LGM).

2 Oceanography

The hydrodynamic system in the Yellow Sea is characterized by two major circulation patterns (Fig. 1). One is a counterclockwise gyre in the western part consisting of the Yellow Sea Warm Current (YSWC) and Yellow Sea Coastal Current (YSCC) (Beardsley et al., 1985; Yang et al., 2003). The other is a clockwise gyre in the eastern part made up of the YSWC and the Korea Coastal Current (KCC) (Beardsley et al., 1985; Yang et al., 2003). The YSWC is one of the most important dynamic phenomena in the East China Sea and Yellow Sea. It is a branch of the Kuroshio Current that carries warm, salty water into the Yellow Sea roughly along the Yellow Sea Trough (Xu et al., 2009; Liu et al., 2010a; Wang et al., 2011, 2012). The YSCC and KCC flow south along the coasts of the China and the Korean Peninsula, respectively. Besides, the Transversal Current (TC), identified in recent studies, separates from the KCC southwest of the Korean Peninsula, and some of its water flows northward along the YSWC (Lie et al., 2013; Hwang et al., 2014; Lie and Cho, 2016) (Fig. 1). On the other hand, freshwater input from the Changjiang to the Yellow Sea forms the plume of low-salinity water, called as the Changjiang Diluted Water (CDW) (Sukigara et al., 2017). A part of the CDW spreads eastward, reaching as far as Jeju Island and the Korea Strait (Hwang et al., 2014; Li et al., 2014a). The oceanic fronts include the Shandong Front (SDF), Jiangsu Coastal Front (JSCF), and Western Korean Coastal Front (WKCF) located in the western and eastern boundaries of the Yellow Sea. These fronts play an important role in shaping Yellow Sea currents and in understanding sediment transport, as they separate different water masses in the center and coast of the Yellow Sea and appear to create a barrier effect for sediment (Huang et al., 2010; Li et al., 2014a; Koo et al., 2018) (Fig. 1).

Table 1. Representative accelerator mass spectrometer radiocarbon age data for core PCL14 from Badejo et al. (2016). OM stands for organic matter.

Core	Depth (cm)	Sample type	^{14}C age (BP)	Age (BP) ±95 % probability
11 YS PCL 14	90	OM	7160 ± 40	8040 ± 90
	300	Shell	10 360 ± 40	12 630 ± 190
	540	Shell	12 400 ± 50	15 030 ± 290
	580	Shell	12 530 ± 50	15 160 ± 210
	698	Shell	12 720 ± 50	15 430 ± 250

3 Materials and methods

Core 11YS-PCL14 (35°785′ N, 124°115′ E), which was 702 cm in length, was collected from CYSM at a water depth of approximately 80 m for multi-proxy paleoenvironmental reconstruction. The core was subsampled at 10 cm intervals for grain size, clay mineralogy, and geochemical analyses. Core 11YS-PCL14 was 702 cm in length and was recovered deeper than other studied cores around in this area (YSC-1; 437 cm, EZ06-1; 370 cm, EZ06-2; 360 cm) (Li et al., 2014a; Lim et al., 2015).

The grain size and accelerator-mass-spectrometer-based ^{14}C dates were reported in Badejo et al. (2016). Radiocarbon ages for five selected depths (99, 300, 540, 580, and 698 cm) and the age–depth model were constructed based on the linear interpolation between the calibrated calendar ages (Badejo et al., 2016) (Table 1). The bottom of the core 11YS-PCL14, dated at approximately 15.5 ka, provides a continuous record from the late last deglaciation to the Holocene in the CYSM.

The clay mineral analysis was conducted using X-ray diffraction (XRD) on preferred-orientation specimens of fine-grained sediment (< 2 µm), following the method in Cho et al. (2015). Semiquantitative estimation of clay mineral abundances was completed using the Eva 3.0 program with the empirical factors from Biscaye (1965).

The composition of major and trace elements in 13 bulk samples was determined by Actlabs (Ontario, Canada), following the "4 LithoRes" methodology. The samples were fused using a lithium metaborate and tetraborate mixture. The melt produced by this process was completely dissolved with 5 % HNO_3. Major elements were analyzed in the resulting solution by inductively coupled plasma optical emission spectrometry (ICP-OES), with an analytical accuracy of < 6 %. Trace element analyses were done by inductively coupled plasma mass spectrometry (ICP-MS). The analytical reproducibility ranged between 5 % and 12 %.

A total 18 samples of core 11YS-PCL14 and riverine sediments (Huanghe, Changjiang and Keum River) were selected for Sr and Nd isotopic analysis and were processed on the < 63 µm fraction of each sample (Table 3). The inorganic silicate fraction was extracted from 18 samples following the method described by Rea and Janecek (1981). The samples were treated with acetic acid buffered to pH 5 with sodium acetate to remove calcium carbonate. They were subsequently treated with a hot sodium citrate and sodium dithionite solution buffered with sodium bicarbonate to remove coarse biogenic components and finally treated with Na_2CO_3 solution to remove biogenic silica. ^{143}Nd/^{144}Nd and ^{87}Sr/^{86}Sr analyses, including chemical separation and multicollector thermal ionization mass spectrometry (VG54-30, Isoprobe-T) analyses, were performed at the Korea Basic Science Institute following Cheong et al. (2013). Sr and Nd isotope ratios were normalized to ^{86}Sr/^{88}Sr = 0.1194 and ^{146}Nd/^{144}Nd = 0.7219, respectively. Analysis of the Sr standard NBS 987 and the Nd standard JNdi-1 resulted in ^{87}Sr/^{86}Sr = 0.710246 ±3 (2 SD, n = 10) and ^{143}Nd/^{144}Nd = 0.512115 ±6 (2 SD, $n = 10$). For convenience, the εNd parameter was calculated using a ^{143}Nd/^{144}Nd value of 0.512638 for the Chondritic Uniform Reservoir ($\varepsilon\text{Nd} = [(^{143}\text{Nd}/^{144}\text{Nd})/0.512638\text{-}1] \times 10^4$) (Hamilton et al., 1983).

4 Results

Core 11YS-PCL14 could be divided mainly into four units considering downcore patterns, especially mean grain size and clay mineral compositions (Figs. 2 and 3): Unit 4 (700–520 cm; 15.5–14.8 ka), Unit 3 (520–310 cm; 14.8–12.8 ka), Unit 2 (310–130 cm; 12.8–8.8 ka), and Unit 1 (130–0 cm; < 8.8 ka). In addition, Unit 2 could be subdivided into Unit 2-2 (310–210 cm; 12.8–10.5 ka) and Unit 2-1 (210–130 cm; 10.5–8.8 ka) based on the variation trends of clay mineral compositions, especially smectite content. The content of smectite increases slightly during the deposition of Unit 2-2 but tends to decrease in Unit 2-1 (Fig. 3). Wang et al. (2014) reported that the CYSM mud blanket becomes thicker in the westward direction based on a seismic profile. The mud layers in core sediments are thinner than expected from the seismic profile, but the trend is consistent (Fig. 2). Core EZ06-2, located east of 11YS-PCL14, contains a 100 cm thick mud layer, while YSC-1 to the west has a 375 cm thick layer (Fig. 2). The lower part of the mud layer is known as the transgressive deposit and contains many sands (Fig. 2). This coarse layer appears in all cores in the CYSM, with a boundary of $\sim$ 10 ka (Li et al., 2014a; Lim et al., 2015). However, core 11YS-PCL14 has additional mud layers with a high proportion of silt underneath the transgressive deposit and a coarse layer at the bottom. Therefore, core 11YS-PCL14 provides more records of the CYSM since the LGM that could not be reconstructed in previous cores (Li et al., 2014a; Lim et al., 2015) because core 11YS-PCL14 was recovered deeper than other studied cores.

The vertical granularity, clay mineralogy, and geochemical characteristics of core 11YS-PCL14 are plotted against the calibrated age on the y axis in Fig. 3. The four clay minerals were dominated by illite (60.1 %–74.7 %), followed by chlo-

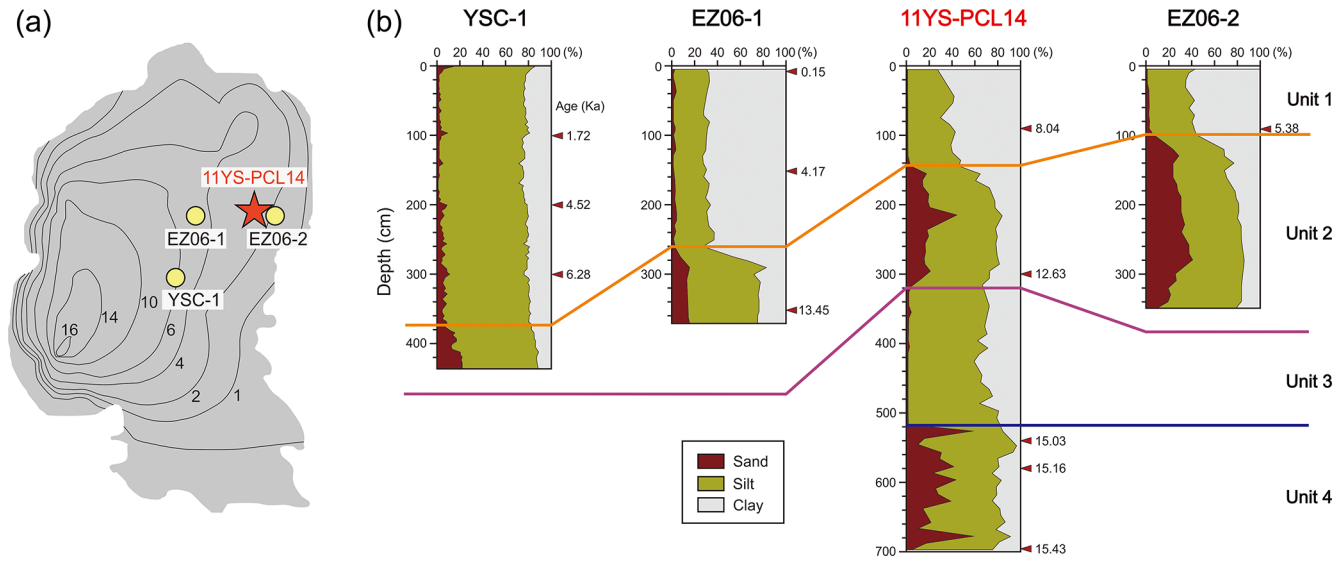

Figure 2. (a) Isolines in thickness (m) of mud deposit CYSM (after Wang et al., 2014). **(b)** Vertical lithology profile of core 11YS-PCL14 and other reference cores (YSC-1, Li et al., 2014a; EZ06-1 and EZ06-2, Lim et al., 2015).

rite (12.0 %–22.6 %), kaolinite (9.6 %–14.8 %), and smectite (1.2 %–6.8 %). The $^{87}Sr/^{86}Sr$ ratios ranged from 0.719 to 0.724 (mean 0.721) and the εNd values from −16.2 to −12.3 (mean −14.0).

Tables 2 and 3 list the detailed characteristics of the clay minerals and geochemistry in each unit and their main potential provenances (the Huanghe, Changjiang, and western Korean rivers). Each unit had distinct dissimilarities in clay mineral content and mean grain size, especially the sand content (Fig. 2). The Unit 2 sediments were 1.8 %–44.2 % (mean 17.6 %) sand with a mean grain size of 6.6 Φ (10.3 µm), and Unit 4 sediments had a high sand content (8 %–58.7 %, mean 26.3 %) with a mean grain size of 6.0 Φ (15.6 µm). In comparison, Unit 1 contained only fine sediment with a mean grain size of 8.8 Φ (2.2 µm), and Unit 3 sediments were clayey silt with a mean grain size of 7.3 Φ (6.3 µm). The downcore variation in the clay mineral composition showed that the illite content decreased gradually from Unit 2 to 3 and was constant in the other parts of the core. Overall, the variation in the smectite and kaolinite+chlorite contents was the opposite of that of illite (Fig. 3). Units 3 and 4 had relatively constant compositions in terms of clay minerals, although their granularity was heterogeneous. The $^{87}Sr/^{86}Sr$ ratio was constant at the bottom and tended to increase in the upper part. The εNd value was low in Units 2 and 4. ΣLREE / ΣHREE (light REE to heavy REE) was low only in Unit 3 and was mostly constant.

5 Discussion

5.1 Provenance discrimination based on clay mineralogy

Relative clay mineral contents and ratios can be used as powerful proxies for determining fine-grained marine sediment provenance, especially in terms of the rivers from China and Korea that may contribute to CYSM (Yang et al., 2003; Choi et al., 2010; Li et al., 2014a; Xu et al., 2014; Lim et al., 2015; Kwak et al., 2016). Generally, Huanghe sediments are characterized by high smectite, and Changjiang sediments contain a lot of illite contents. Western Korean rivers (e.g., the Han, Keum, and Yeongsan) contain more kaolinite and chlorite than do Chinese rivers (Table 2).

A ternary diagram of smectite-(kaolinite + chlorite)-illite is utilized to determine the provenance of fine sediments in core 11YS-PCL14 (Fig. 4). Although Unit 4 and Unit 3 sediments differed in granularity, they had similar clay mineral compositions and plotted near the center of the three possible provenance end-members, indicating that fine-grained sediments were supplied with constant amounts from all potential rivers to the study area during these periods (Fig. 4a). Unit 2 sediments overall were characterized by an increasing illite content (Figs. 3 and 4b). It means that the influence of Changjiang-derived materials began to increase during this period. However, Unit 2-2 sediments displayed an increase in smectite content with illite, and clay mineral compositions other than illite decrease in Unit 2-1 (Fig. 4b). Variation of smectite content in Unit 2 appears to be closely related to the change in coarse sediments (Figs. 3 and 4b). The relationship between smectite and coarse grains was also observed in the early Holocene sedimentary unit of core YSC-1 (Li

Table 2. Average compositions of clay minerals in core 11YS-PCL14 sediments and their potential provenance rivers.

Samples	*n*	Illite (%)	Chlorite (%)	Kaolinite (%)	Smectite (%)	Reference
11YS-PCL14_Unit 1	9	69.0 ± 1.6	18.2 ± 1.3	10.9 ± 0.6	1.8 ± 0.4	This study
11YS-PCL14_Unit 2	16	67.0 ± 3.0	16.5 ± 2.3	12.1 ± 1.2	4.5 ± 1.1	
11YS-PCL14_Unit 3	24	63.0 ± 1.1	19.7 ± 1.0	13.7 ± 0.6	3.6 ± 0.5	
11YS-PCL14_Unit 4	18	63.2 ± 1.4	20.0 ± 1.3	13.0 ± 0.7	3.8 ± 0.7	
Changjiang	9	68.1	17.0	13.3	1.6	Koo et al. (2018)
	8	66	12	16	6	Yang et al. (2003)
	–	61.7	24.5	9.8	3.9	Choi et al. (2010)
Huanghe	13	62.2	15.8	13.1	8.9	Koo et al. (2018)
	4	56.7	17.7	14.1	11.5	Cho et al. (2015)
	8	62	16	10	12	Yang et al. (2003)
Western Korean rivers	14/9/3	59.5	21.3	17.4	1.8	Cho et al. (2015)
(Han/Keum/Yeongsan)	45	52	44		4	Lim et al. (2015)

Table 3. Isotopic and geochemical data of core PCL14 and riverine samples.

Samples	$^{87}Sr/^{86}Sr$ ($\pm 2\sigma \times 10^6$)	$^{143}Nd/^{144}Nd$ ($\pm 2\sigma \times 10^6$)	εNd	(La/Yb) ucc	(La/Lu) ucc	ΣLREE/ ΣHREE	ΣLREE/ Yb
PCL14-2 (47 cm)	0.722591 (14)	0.511999 (4)	−12.5	1.09	1.08	4.07	63.1
PCL14-4 (67 cm)	0.723603 (11)	0.511988 (5)	−12.7	1.18	1.11	4.09	68.1
PCL14-8 (107 cm)	0.720661 (11)	0.511971 (4)	−13.0	1.18	1.14	4.2	68.1
PCL14-11 (137 cm)	0.723536 (17)	0.511880 (3)	−14.8	1.2	1.15	4.18	70.5
PCL14-17 (197 cm)	0.719741 (11)	0.511860 (3)	−15.2	1.2	1.09	4.21	69.5
PCL14-25 (277 cm)	0.719819 (14)	0.511908 (3)	−14.2	1.15	1.07	4.06	65.8
PCL14-30 (327 cm)	0.718528 (27)	0.512010 (3)	−12.3	1.01	0.99	3.64	58.5
PCL14-37 (397 cm)	0.720141 (7)	0.511980 (4)	−12.8	1.12	1.04	3.75	64.8
PCL14-42 (447 cm)	0.720495 (50)	0.511965 (7)	−13.1	1.07	1.01	3.77	62.7
PCL14-54 (567 cm)	0.720030 (8)	0.511883 (6)	−14.7	1.17	1.10	4.09	67.5
PCL14-60 (627 cm)	0.720886 (8)	0.511808 (10)	−16.2	1.12	1.04	3.96	65.1
PCL14-67 (697 cm)	0.719559 (8)	0.511817 (5)	−16.0	1.19	1.18	4.09	67.4
Huanghe	0.717596 (9)	0.512073 (5)	−11.0				
	0.717260 (10)	0.512063 (4)	−11.2				
Changjiang	0.722954 (8)	0.511999 (6)	−12.5				
	0.726349 (7)	0.512018 (5)	−12.1				
Keum River	0.724526 (6)	0.511609 (4)	−20.1				
	0.724881 (5)	0.511700 (3)	−18.3				

et al., 2014a) and the nearby core EZ06-2 between ∼ 14.1 and ∼ 9.0 ka (Lim et al., 2015). Unit 1 sediments had clay mineral compositions quite similar to those of Changjiang sediments, indicating that they might be originate mainly from the Changjiang (Fig. 4b). Consequently, clay mineralogical results suggest that the provenance of fine-grained sediments are changed according to each unit as follows: fine-grained sediments during the depositions of Unit 3 and 4 were supplied from all potential provenances, the influence of the Changjiang increased gradually during the deposition of Unit 2, and Unit 1 sediments were mainly originated from the Changjiang.

5.2 Provenance discrimination based on geochemistry

Geochemical proxies for provenance discrimination in the Yellow Sea have been investigated actively and verified by several studies (e.g., Yang et al., 2002; Xu et al., 2009; Song and Choi, 2009; Jung et al., 2012; Ha et al., 2013; Lim et al., 2015; Hu et al., 2018; Koo et al., 2018). The chemical compositions of Korean and Chinese rivers differ, especially in their rare earth elements (REEs) and Sr and Nd contents (Xu et al., 2009; Jung et al., 2012; Lim et al., 2014; Hu et al., 2018). The trace elements and isotopes are essentially unaltered during weathering, transport, and sedimentation, and can be a powerful tool for tracing the provenance of the

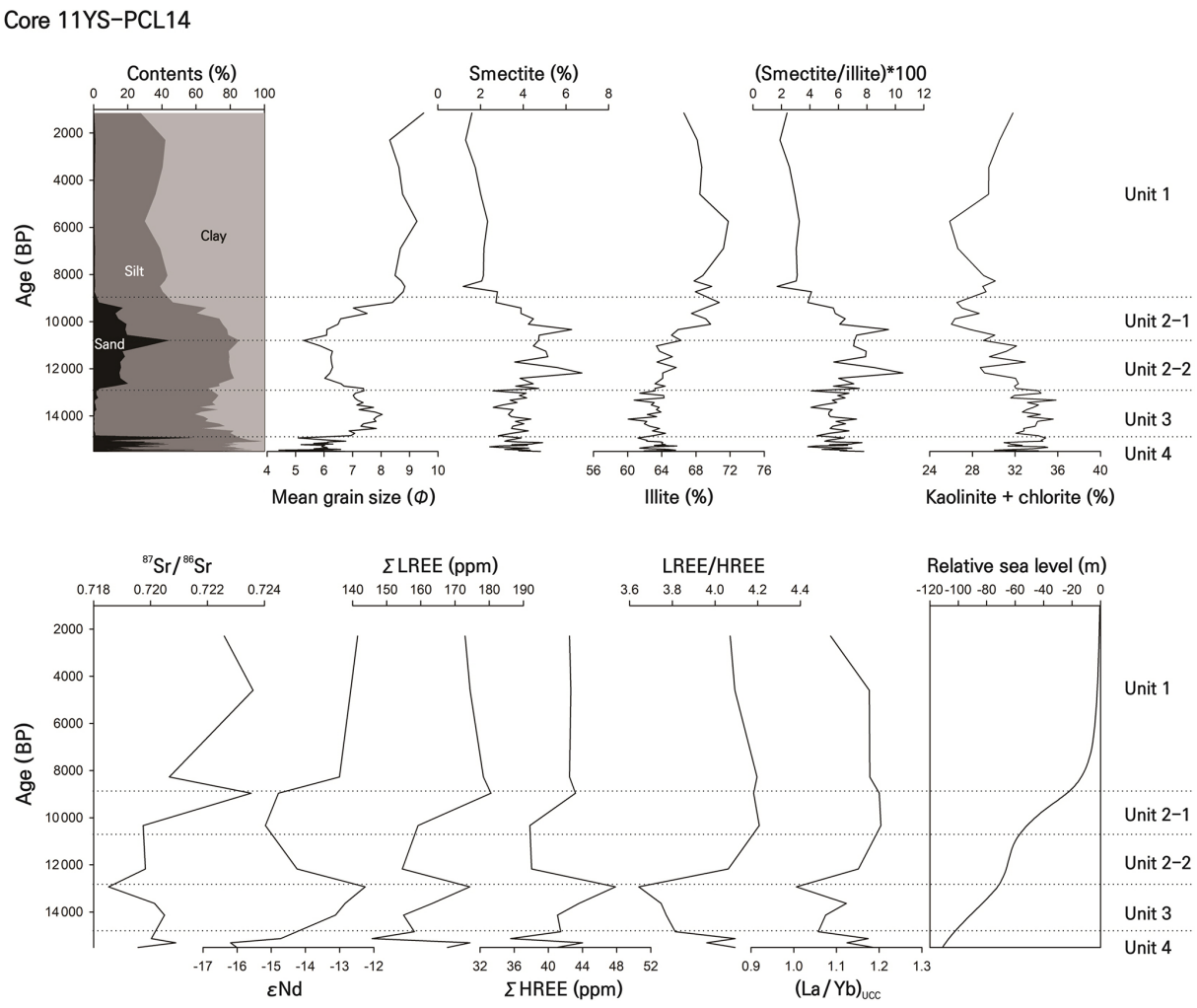

Figure 3. Downcore variations of mean grain size and clay mineralogical and geochemical data in core 11YS-PCL14 with sea level changes (Li et al., 2014b). Note the overall distribution into four units.

terrigenous fraction of marine sediments (McLennan, 1989; Blum and Erel, 2003; Xu et al., 2009; Chaudhuri et al., 2020).

Recent studies have emphasized caution relating to misinterpretation of sediment provenance due to other factors that influence the geochemical composition of riverine and marine sediments, such as grain size and biogenic component (Yang et al., 2002; Song and Choi, 2009; Lim et al., 2015; Hu et al., 2018). For example, the major elements Fe and Mg, as well as some trace elements, have been proposed as being useful as provenance indicators in the Yellow Sea (Song and Choi, 2009; Koo et al., 2018), but they are closely correlated with particle size, which can lead to misinterpretation of sediment provenance (Fig. 5a). In addition, Ca has a problem based on biogenic carbonate despite its poor correlation with grain size (Fig. 5a). To complement the grain size effect, recent studies have suggested ratios of the binding of abundant elements at comparable grain sizes (e.g., the La/Sc and Zr/Th ratios) (Yang et al., 2002; Lim et al., 2014). However, we observed that these ratios and mean grain size were strongly negatively correlated in our dataset (Fig. 5b), implying that these ratios are also unsuitable for studying provenance. Normalization of REE values to upper continental crust (UCC) is a widely accepted method for discriminating the sediment provenances of various geological materials (Taylor and McLennan, 1985; Song and Choi, 2009; Xu et al., 2009; Lim et al., 2015). This method can better offset differences caused by grain size and could be a useful geochemical proxy (Fig. 5c). In addition, the Nd isotope ratio of silicate particles is essentially unaltered during weathering, transport, and sedimentation and can be a powerful tool for tracing the provenance of the terrigenous fraction of marine sediments (Blum and Erel, 2003; Hu et al., 2018). However, recent studies indicated that the Sr isotope composition in both Chinese and Korean riverine sediments was a function of grain size, with a higher $^{87}Sr/^{86}Sr$ in clay-dominated fractions than in silt-dominated fractions (Fig. 5d) (Hu et al.,

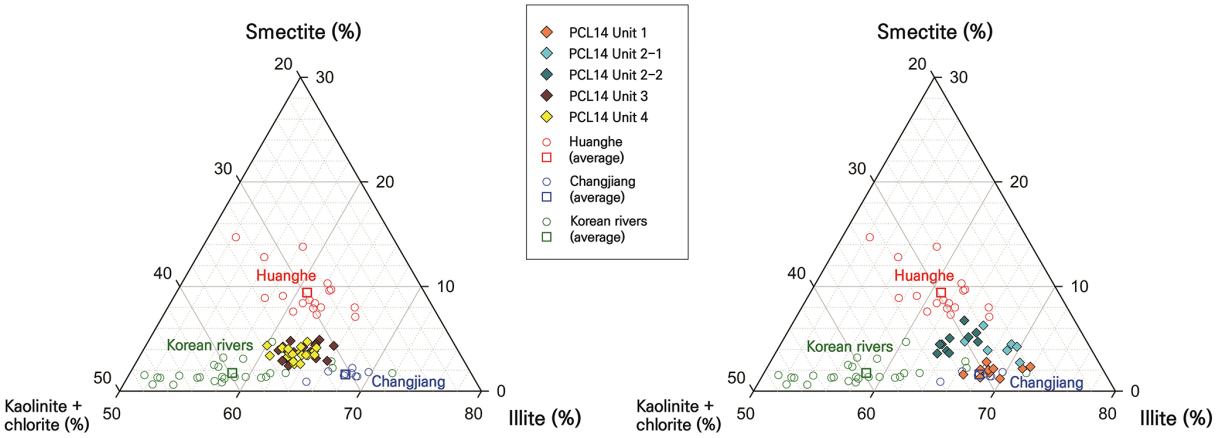

Figure 4. Ternary diagrams showing variations in clay mineral compositions of core 11YS-PCL14. Published data of potential source sediments, including the Changjiang, Huanghe, and western Korean rivers (the Han, Keum, and Yeongsan rivers) (Cho et al., 2015; Koo et al., 2018), which are plotted for comparison.

2018). For these reasons, we used only the UCC-normalized REE and Nd isotope, independent of grain size effect, to distinguish sediment provenance.

Korean rivers are characterized by a high LREE and low εNd, while Chinese rivers have abundant MREE (middle REE) and high εNd (Table 3, Fig. 6). Figure 6 shows discrimination plots using the REE and εNd values that clearly separate the Chinese and Korean rivers. The REE and εNd values in these plots could represent the source of all sediments including coarse and fine sediments because the REE analysis was performed using the bulk powder samples. Unit 1 sediments are generally close to the Changjiang, which is consistent with results in clay mineralogy (Figs. 4 and 6). Unit 4 sediments are plotted between Chinese and Korean river end-members in all discrimination plots (Fig. 6), consistent with the results for clay minerals, which suggests that the coarse sediments included in Unit 4 were from contributions from all potential rivers.

Interestingly, the fine-grained sediments of Unit 2 were a composite of the Huanghe and Changjiang in Fig. 4, but the geochemical data were similar to Unit 4 (Fig. 6). This probably means that a significant amount of coarse sediments in Unit 2 was supplied from Korean rivers with a high LREE (Fig. 6a). The results of the isotope analysis in the core YSC-1 also showed an increased impact of Korean rivers and coarse sediments before $\sim$ 8 ka, which is consistent with our results (Hu et al., 2018). Thus, the supply of smectite in fine-grained sediments and sand grains is synchronic but possibly has different sources. In addition, Unit 3 sediments, identified as the homogenous origin of Unit 4 in clay mineralogy (Fig. 4), are biased towards Chinese rivers (Fig. 6), especially close to the Huanghe. A scatterplot of clay mineral ratio vs. εNd distinguished three possible provenances for particles smaller than 63 µm (Fig. 6c). Unit 3 sediments in this plot are certainly plotted close to the Huanghe, which is different distribution than previous plots.

This result is likely to be due to the influence of silt-sized particles, which is not considered in clay mineralogy, because Unit 3 sediments contain a large amount of silt content (Fig. 2). Therefore, fine-grained sediments were supplied from all rivers to the study area, but coarse-grained sediments appear to have been mainly sourced from the Huanghe during the deposition of Unit 3 (Figs. 4 and 6). Consequently, the estimated sediment provenances in each unit based on the clay mineralogical and geochemical indices were as follows. During the deposition of Unit 4, both coarse and fine sediments were influenced by all of these provenances. However, in Unit 3, silt-sized fractions were predominantly affected by the Huanghe. Unit 2 represented a period of great change in the sediment sources. The fine grains in the Unit 2-2 sediments were derived primarily from Chinese rivers, especially the Huanghe, while the Unit 2-1 samples were supplied mainly from the Changjiang, with minor contributions from the Huanghe and western Korean rivers. However, the coarse sediments sources in Unit 2 were identified as western Korean rivers, based on geochemical indices. The source of CYSM sediments in Unit 1 was primarily the Changjiang.

5.3 Paleo-environmental implications for sediment provenance changes

The four units could be distinguished based on the characterization of the major sediment source changes in the CYSM over the last 15.5 kyr (Figs. 4–6). Identification of sediment sources is a useful method for understanding paleo-environmental dynamics and sediment transport mechanisms in the Yellow Sea since the late last deglaciation. The main factors that potentially influenced provenance changes in the Yellow Sea include pronounced sea level fluctuations that regulate the positions of shorelines, paleo-river pathways,

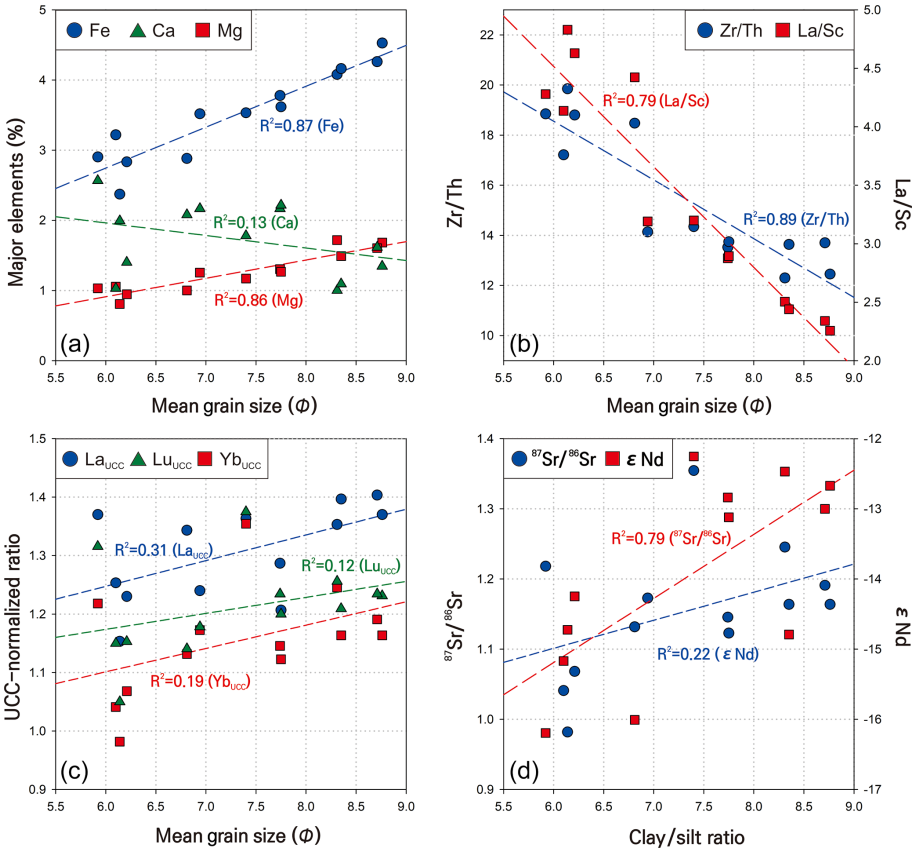

Figure 5. Correlation plots of grain size or clay/silt ratio with **(a)** major elements, **(b)** Zr/Th and La/Sc, **(c)** Upper Continental Crust (UCC)-normalized REEs (Taylor and McLennan, 1985), and **(d)** $^{87}Sr/^{86}Sr$ and εNd for core 11YS-PCL14.

tidal stress amplitude, and the formation of modern ocean currents (Liu et al., 2004; Lim et al., 2007, 2015; Choi et al., 2010; Wang et al., 2014; Yoo et al., 2015, 2016). Here, we discuss how these complex processes have affected sedimentation in the CYSM during the last 15.5 kyr.

The sea level during the depositions of Units 3 and 4, which corresponds to the late last deglaciation (15.5–12.8 ka), was approximately 60–100 m lower than the present sea level (Li et al., 2014b). The high signatures of C/N values in Unit 4 indicated a significant influx of terrigenous materials (Badejo et al., 2016). Mixed deposits of fine and coarse sediments with high influx and sedimentation rates (Figs. 2 and 3) allows us to infer Unit 4 as a delta or prodelta environment. The paleo-river pathways of potential provenances, recently reconstructed based on seismic profiles, merged around the study area and were connected to the East China Sea (Yoo et al., 2015, 2016). During sedimentation of Unit 4, sediments in the study area would have been affected most strongly by direct inflow from paleo-rivers because the low sea level led to the exposure of shelves in and near the Yellow Sea (Li et al., 2014b).

Sediment becoming finer during the deposition of Unit 3 reflects an increase in distance between the river mouths and study area due to transgression, and the study area probably formed a mud flat during sedimentation of Unit 3. During this period, fine-grained sediments were supplied from all rivers (Fig. 4), while silt-sized particles were supplied mainly from the Huanghe (Figs. 4 and 6). The record for the same period in core EZ06-1 shows significant coarse sediments with a high sand content (Lim et al., 2015), indicating that the Huanghe was relatively close to the west side of the study area (Fig. 2). In addition, the substantial flux from the Huanghe would have supported the distant movement of coarse grains.

In Unit 2 (12.81–8.8 ka), corresponding to the early Holocene, the sea level was approximately 20–60 m lower than at present (Li et al., 2014b). The Unit 2 period was thought to be cold and dry (Badejo et al., 2016) and was characterized by oscillating grain sizes and clay mineral and geochemical compositions (Fig. 3). In addition, increasing and decreasing trends of grain size with sand content divided the S/I ratio into two subsections (Fig. 3). This variation is also reported in the surrounding YSC-1 (Li et al., 2014a) EZ06-1, and EZ06-2 cores. In this period, the low sea level led to the seaward progradation of the shoreline and formation of a thin sand layer (generally < 3 m) called

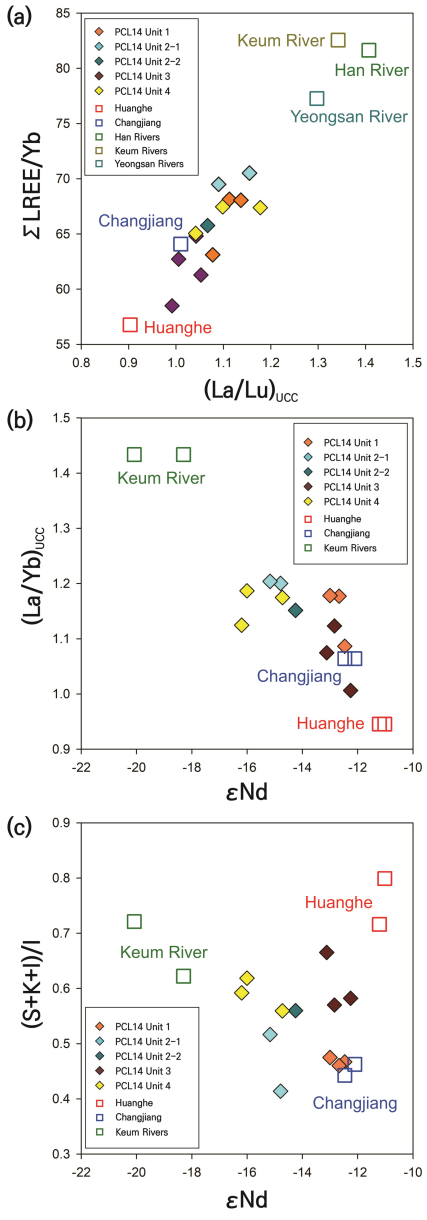

Figure 6. Discrimination plots showing variations in **(a)** $\sum$LREE / Yb vs. $(La/Lu)_{UCC}$, **(b)** $(La/Yb)_{UCC}$ vs. εNd, and **(c)** (smectite + kaolinite + chlorite)/illite vs. εNd. Clay mineral (Cho et al., 2015; Koo et al., 2018), rare earth element (Xu et al., 2009), and isotope data of potential sources are also shown for comparison.

the transgressive deposit throughout the Yellow Sea (Cummings et al., 2016). The change in the coastline configuration caused shifts of the tidal fields therein, with tidal currents being more energetic than at present (Uehara and Saito, 2003; Lim et al., 2015), which supplied coarse grains to the central Yellow Sea. In addition, the bottom stress in the Unit 2 period was stronger around the Korean Peninsula (Uehara and Saito, 2003), which caused most of the coarse sediment to be of western Korean river origin (Fig. 6). The supply of fine sediments from the Huanghe was temporarily strengthened during sedimentation of Unit 2-2 but weakened in Unit 2-1 (Fig. 4). This could be due to a change in distance between the Huanghe and the study area as the sea level rose. In addition, the paleo-Changjiang Shoal moved northeastward into the Yellow Sea at $\sim$ 12 ka (Li et al., 2000) and may have contributed some materials to the study area (Lim et al., 2015). The reduction in Huanghe-derived materials due to the increased distance could be strengthen the influence of the Changjiang in Unit 2-1.

Since sedimentation of Unit 1 ($<$ 8.8 ka), the sea level rose slowly from -20 m to the present level (Li et al., 2014b). The tidal field of the Yellow Sea became similar to that of the present (Uehara and Saito, 2003), leading to obviously decreasing contributions from sea bed erosion. A modern-type circulation in the Yellow Sea may have developed between 8.47 and 6.63 ka, characterized by an increase in bottom-water salinity (Kim and Kucera, 2000). The clay minerals and geochemical composition generally point to the Changjiang, with minor influence from the western Korean rivers (Figs. 4 and 6), which is consistent with the reported "multiple origin" concept (Wei et al., 2003; Li et al., 2014a; Lim et al., 2015; Koo et al., 2018). Therefore, the formation of the CYSM and modern ocean circulation could have been synchronic around $\sim$ 8 ka. The timing of mud patch formation in the central Yellow Sea was inferred to be 9–8 ka with low tidal bottom stress (0.35 N m^{-2}) (Uehara and Saito, 2003), which is consistent with our results.

The YSWC played a major role in the unique passage of sediment into the study area since the Unit 1 (Li et al., 2014a; Lim et al., 2015; Koo et al., 2018). The Changjiang Diluted Water can spread some finer sediments to Jeju and nearby areas (Hwang et al., 2014; Li et al., 2014a; Lim et al., 2015; Kwak et al., 2016; Koo et al., 2018). Following this, fine-grained materials could be carried northward along the YSWC path to the CYSM, where the weak tidal-current system and cyclonic eddies provided favorable environment for the formation and maintenance of muddy sediment (Shi et al., 2003; Lim et al., 2015). Meanwhile, the barrier effect of oceanic fronts and strong coastal currents restricts the entrance of sediments from the Huanghe and western Korean rivers into the CYSM (Li et al., 2014a; Koo et al., 2018). However, some fine-grained particles from western Korean rivers may influence the CYSM through the Transversal Current (Hwang et al., 2014; Koo et al., 2018).

6 Conclusions

The purpose of this study was to better understand the CYSM in terms of provenance changes and transport mechanisms and to reconstruct the paleo-environment of the Yellow Sea since the late last deglaciation using clay mineralogy and

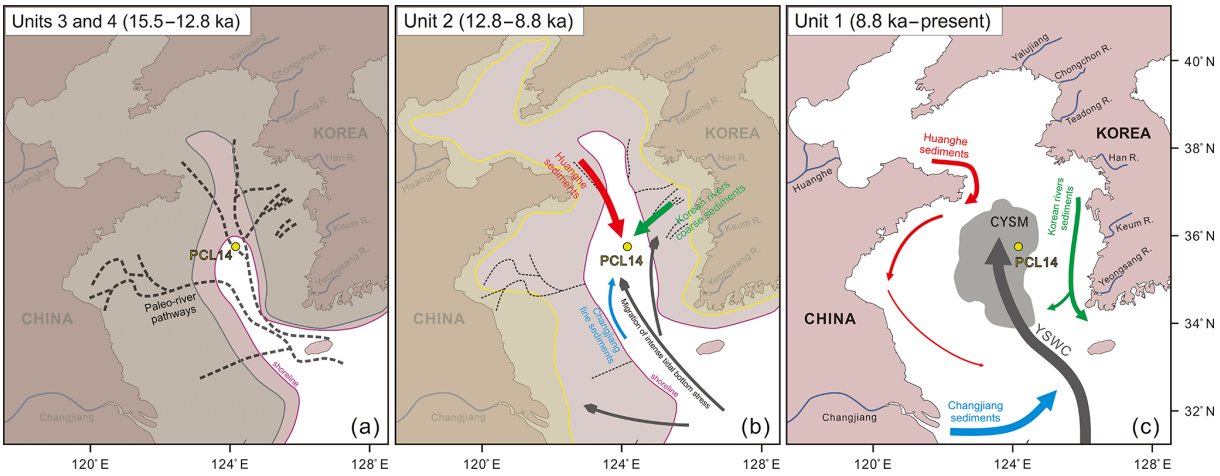

Figure 7. Schematic diagram showing the influence of shoreline changes and paleo-river pathways on riverine sediment supplied to the study area during **(a)** Unit 4 and 3 (15.5–12.8 ka), **(b)** Unit 2 (12.8–8.8 ka), and **(c)** Unit 1 (8.8 ka–present) (modified Lim et al., 2015)

geochemical indices from core 11YS-PCL14. The major conclusions are as follows.

Core 11YS-PCL14 provides a continuous record of the late last deglaciation to Holocene in the CYSM. The core could be divided mainly into four units: Unit 4 (700–520 cm; 15.5–14.8 ka), Unit 3 (520–310 cm; 14.8–12.8 ka), Unit 2 (310–130 cm; 12.8–8.8 ka), and Unit 1 (130–0 cm; < 8.8 ka). Unit 2 is divided into two subunits, Unit 2-2 (310–210 cm; 12.8–10.5 ka) and Unit 2-1 (210–130 cm; 10.5–8.8 ka), according to smectite content.

The integration of clay mineralogical and geochemical data distinguished the CYSM sediments into different provenances by grain size. During the deposition of Unit 4, fine and coarse sediments were supplied from all possible rivers in the Korea and China by direct inflow from paleo-rivers with the exposure of shelves. Sediment fining in the Unit 3 reflects an increase in distance between the river mouths and study area. In this period, fine-grained sediments were still supplied from all rivers, while silt-sized particles were supplied mainly from the Huanghe. During the deposition of Unit 2, the bottom stress was stronger around the Korean Peninsula, which caused most of the coarse sediment to be of western Korean river origin. However, the supply of fine sediments from the Huanghe temporarily strengthened in the Unit 2-2, but weakened in Unit 2-1, due to a change in distance between the Huanghe and the study area as the sea level rose. Unit 1 sediments were composed mainly of sources from the Changjiang. After the oceanic circulation was formed, the YSWC played a major role in the unique passage of sediment into the study area. In addition, the barrier effect of oceanic fronts and strong coastal currents restricts the entrance of the sediments from the Huanghe and western Korean rivers into the study area.

Data availability. A dataset related to core 11YS-PCL14 is available from the Supplement.

Supplement. The supplement related to this article is available online at: https://doi.org/10.5194/os-16-1247-2020-supplement.

Author contributions. HGC designed the experiments, and HJK carried them out and wrote the paper. Both of the authors contributed to interpreting and discussing the results and reviewing the paper.

Competing interests. The authors declare that they have no conflict of interest.

Acknowledgements. This study was supported by the Basic Science Research Program through the National Research Foundation of Korea (NRF), funded by the Ministry of Education, Science and Technology (2017R1D1A1B03027818), and the Korea Polar Research Institute (project no. PM16050), funded by the Ministry of Oceans and Fisheries, Korea.

Financial support. This research has been supported by the National Research Foundation of Korea (grant no. 2017R1D1A1B03027818) and the Korea Polar Research Institute (grant no. PM16050).

Review statement. This paper was edited by Arvind Singh and reviewed by Neeraj Awasthi, Sonal Khanolkar, and one anonymous referee.

References

Badejo, A. O., Choi, B.-H., Cho, H.-G., Yi, H.-I., and Shin, K.-H.: Environmental change in Yellow Sea during the last deglaciation to the early Holocene (15,000-8,000 BP), Quat. Int., 392, 112–124, https://doi.org/10.1016/j.quaint.2015.07.060, 2016.

Beardsley, R. C., Limeburner, R., Yu, H., and Cannon, G.A.: Discharge of the Changjiang (Yangtze River) into the East China Sea, Cont. Shelf Res., 4, 57–76, https://doi.org/10.1016/0278-4343(85)90022-6, 1985.

Biscaye, P. E.: Mineralogy and sedimentation of recent deep-sea clay in the Atlantic Ocean and adjacent seas and oceans, Geol. Soc. Am. Bull., 76, 803–832, https://doi.org/10.1130/0016-7606(1965)76[803:MASORD]2.0.CO;2, 1965.

Blum, J. and Erel, Y.: Radiogenic isotopes in weathering and hydrology, Treatise on Geochemistry, 5, 365–392. https://doi.org/10.1016/B0-08-043751-6/05082-9, 2003.

Chaudhuri, A., Banerjee, S., and Chauhan, G.: Compositional evolution of siliciclastic sediments recording the tectonic stability of a pericratonic rift: Mesozoic Kutch Basin, western India, Mar. Petrol. Geol., 111, 476–495, 2020.

Cheong, C.-S., Ryu, J.-S., and Jeong, Y.-J.: Simultaneous multiple collector-ICP-MS measurement of Nd isotopic composition and Sm/Nd ratio in geological reference materials by interference corrections and external calibration using matrix-matched standards, Geosci. J., 17, 389–395, https://doi.org/10.1007/s12303-013-0056-5, 2013.

Cho, H. G., Kim, S.-O., Kwak, K. Y., and Choi, H.: Clay mineral distribution and provenance in the Heuksan mud belt, Yellow Sea, Geo-Mar. Lett., 35, 411–419, https://doi.org/10.1007/s00367-015-0417-3, 2015.

Choi, J. Y., Lim, D. I., Park, C. H., Kim, S. Y., Kang, S., and Jung, H. S.: Characteristics of clay mineral compositions in river sediments around the Yellow Sea and its application to the provenance of the continental shelf mud deposit, J. Geol. Soc. Korea, 46, 497–509, 2010.

Cummings, D., Dalrymple, R., Choi, K., and Jin, J.: The Tide-Dominated Han River Delta, Korea: Geomorphology, Sedimentology, and Stratigraphic Architecture, Elsevier, Amsterdam, 382 pp, 2016.

Duck, R. W., Rowan, J. S., Jenkins, P. A., and Youngs, I.: A multi-method study of bed load provenance and transport pathways in an estuarine channel, Phys. Chem. Earth, 26, 747–752, https://doi.org/10.1016/S1464-1909(01)00080-6, 2001.

Dou, Y., Yang, S., Liu, Z., Chlift, P. D., Yu, H., Berne, S., and Shi, X.: Clay mineral evolution in the central Okinawa Trough since 28 ka: implications for sediment provenance and paleoenvironmental change, Palaeogeogr. Palaeoclimatol. Palaeoecol., 288, 108–117, https://doi.org/10.1016/j.palaeo.2010.01.040, 2010.

Ha, H. J., Chun, S. S., and Chang, T. S.: Distribution pattern, geochemical composition, and provenance of the Huksan Mud Belt Sediments in the Southeastern Yellow Sea, J. Korean Earth Sci. Soc., 34, 289–302, https://doi.org/10.5467/JKESS.2013.34.4.289, 2013.

Hamilton, P., O'nions, R., Bridgwater, D., and Nutman, A.: Sm–Nd studies of Archaean metasediments and metavolcanics from West Greenland and their implications for the Earth's early history, Earth Planet. Sci. Lett., 62, 263–272, https://doi.org/10.1016/0012-821X(83)90089-4, 1983.

Hu, B. Q., Yang, Z. S., Zhao, M. X., Saito, Y., Fan, D. J., and Wang, L. B.: Grain size records reveal variability of the East Asian Winter Monsoon since the Middle Holocene in the Central Yellow Sea mud area, Sci. China Earth Sci., 55, 1656–1668, https://doi.org/10.1007/s11430-012-4447-7, 2012.

Hu, B., Li, J., Zhao, J., Yan, H., Zou, L., Bai, F., Xu, F., Yin, X., and Wei, G.: Sr–Nd isotopic geochemistry of Holocene sediments from the South Yellow Sea: Implications for provenance and monsoon variability, Chem. Geol., 479, 102–112, https://doi.org/10.1177/0959683614540963, 2018.

Huang, D., Zhang, T., and Zhou, F.: Sea-surface temperature fronts in the Yellow and East China Seas from TRMM microwave imager data, Deep-Sea Res. Pt. II, 57, 1017–1024, https://doi.org/10.1016/j.dsr2.2010.02.003, 2010.

Hwang, J. H., Van, S. P., Choi, B.-J., Chang, Y. S., and Kim, Y. H.: The physical processes in the Yellow Sea, Ocean Coastal Manage., 102, 449–457, https://doi.org/10.1016/j.ocecoaman.2014.03.026, 2014.

Jung, H.-S., Lim, D., Choi, J.-Y., Yoo, H.-S., Rho, K.-C., and Lee, H.-B.: Rare earth element compositions of core sediments from the shelf of the South Sea, Korea: Their controls and origins, Cont. Shelf Res., 48, 75–86, https://doi.org/10.1016/j.csr.2012.08.008, 2012.

KIGAM (Korea Institute of Geology, Mining and Materials): Marine geological study of the continental shelf off Kunsan, West Coast, Korea, KIGAM Technical Report KR-93-5A, Daejeon, Korea, 261 pp, 1993.

Kim, J.-M. and Kucera, M.: Benthic foraminifer record of environmental changes in the Yellow Sea (Hwanghae) during the last 15 000 years, Quat. Sci. Rev., 19, 1067–1085, https://doi.org/10.1016/S0277-3791(99)00086-4, 2000.

Koo, H. J., Lee, Y. J., Kim, S. O., and Cho, H. G.: Clay mineral distribution and provenance in surface sediments of Central Yellow Sea Mud, Geosci. J., 22, 989–1000, https://doi.org/10.1007/s12303-018-0019-y, 2018.

Kwak, K. Y., Choi, H., and Cho, H.G.: Paleo-environmental change during the late Holocene in the southeastern Yellow Sea, Korea, Appl. Clay Sci., 134, 55–61, https://doi.org/10.1016/j.clay.2016.05.007, 2016.

Lee, H. J. and Chough, S. K.: Sediment distribution, dispersal and budget in the Yellow Sea, Mar. Geol., 87, 195–205, https://doi.org/10.1016/0025-3227(89)90061-3, 1989.

Li, C. X., Chen, Q. Q., Zhang, J. Q., Yang, S. Y., and Fan, D. D.: Stratigraphy and paleoenvironmental changes in the Yangtze Delta during the Late Quaternary, J. Asian Earth Sci., 18, 453–469, https://doi.org/10.1016/S1367-9120(99)00078-4, 2000.

Li, J., Hu, B. Q., Wei, H. L., Zhao, J. T., Zou, L., Bai, F. L., Dou, Y. U., Wang, L. B., and Fang, X. S.: Provenance variations in the Holocene deposits from the southern Yellow Sea: clay mineralogy evidence, Cont. Shelf Res., 90, 41–51, https://doi.org/10.1016/j.csr.2014.05.001, 2014a.

Li, G., Li, P., Liu, Y., Qiqo, L., Ma, Y., Xu, J., and Yang, Z.: Sedimentary system response to the global sea level change in the East China Seas since the last glacial maximum, Earth-Sci. Rev. 139, 390–405, https://doi.org/10.1016/j.earscirev.2014.09.007, 2014b.

Lie, H.-J., Cho, C.-H., and Lee, S.: Frontal circulation and westward transversal current at the Yellow Sea entrance

in winter, J. Geophys. Res.-Oceans, 118, 3851–3870, https://doi.org/10.1002/jgrc.20280, 2013.

Lie, H.-J. and Cho, C.-H.: Seasonal circulation patterns of the Yellow and East China Seas derived from satellite-tracked drifter trajectories and hydrographic observations, Prog. Oceanogr., 146, 121–141, https://doi.org/10.1016/j.pocean.2016.06.004, 2016.

Lim, D. J., Choi, J. Y., Jung, H. S., Rho, K. C., and Ahn, K. S.: Recent sediment accumulation and origin of shelf mud deposits in the Yellow and East China Seas, Prog. Oceanogr., 73, 145–159, https://doi.org/10.1016/j.pocean.2007.02.004, 2007.

Lim, D., Jung, H. S., and Choi, J. Y.: REE partitioning in riverine sediments around the Yellow Sea and its importance in shelf sediment provenance, Mar. Geol., 357, 12–24, https://doi.org/10.1016/j.margeo.2014.07.002, 2014.

Lim, D. I., Xu, Z. K., Choi, J. Y., Li, T. G., and Kim, S. Y.: Holocene changes in detrital sediment supply to the eastern part of the central Yellow Sea and their forcing mechanisms, J. Asian Earth Sci., 150, 18–31, https://doi.org/10.1016/j.jseaes.2015.03.032, 2015.

Liu, J. P., Milliman, J. D., and Gao, S.: The Shandong mud wedge and post-glacial sediment accumulation in the Yellow Sea, Geo-Mar. Lett., 21, 212–218, https://doi.org/10.1007/s00367-001-0083-5, 2002.

Liu, J. P., Milliman, J. D., Gao, S., and Cheng, P.: Holocene development of the Yellow River's subaqueous delta, North Yellow Sea, Mar. Geol., 209, 45–67, https://doi.org/10.1016/j.margeo.2004.06.009, 2004.

Liu, J., Saito, Y., Wang, H., Yang, Z., and Nakashima, R.: Sedimentary evolution of the Holocene subaqueous clinoform off the Shandong Peninsula in the Yellow Sea, Mar. Geol., 236, 165–187, https://doi.org/10.1016/j.margeo.2006.10.031, 2007.

Liu, J., Saito, Y., Kong, X., Wang, H., Wen, C., Yang, Z., and Nakashima, R.: Delta development and channel incision during marine isotope stage 3 and 2 in the western South Yellow Sea, Mar. Geol., 278, 54–76, https://doi.org/10.1016/j.margeo.2010.09.003, 2010a.

Liu, Z., Colin, C., Li, X., Zhao, Y., Tuo, S., Chen, Z., Siringan, F. P., Liu, J. T., Huang, C.-Y., You, C.-F., You, C.-F., and Huang, K.-F.: Clay mineral distribution in surface sediments of the northeastern South China Sea and surrounding fluvial drainage basins: Source and transport, Mar. Geol., 277, 48–60, https://doi.org/10.1016/j.margeo.2010.08.010, 2010b.

McLennan, S. M.: Rare earth elements in sedimentary rocks: influence of provenance and sedimentary processes, in: Geochemistry and mineralogy of rare earth elements, edited by: Lipin, B. R. and McKay, G. A., Reviews in Mineralogy, 21, Mineralogy Society of America, Washington, DC, 169–200, 1989.

Milliman, J. D., Shen, H. T., Yang, Z. S., and Mead, R. H.: Transport and deposition of river sediment in the Changjiang estuary and adjacent continental shelf, Cont. Shelf Res., 4, 37–45, https://doi.org/10.1016/0278-4343(85)90020-2, 1985.

Milliman, J. D., Qin, Y. S., Ren, M. E., and Saito, Y.: Man's influence on the erosion and transport of sediment by Asian rivers: the Yellow River (Huanghe) example, J. Geol., 95, 751–762, https://doi.org/10.1086/629175, 1987.

Rea, D. K. and Janecek, T. R.: Late cretaceous history of eolian deposition in the mid-pacific mountains, central North Pacific Ocean, Palaeogeogr. Palaeoclimatol. Palaeoecol., 36, 55–67, https://doi.org/10.1016/0031-0182(81)90048-1, 1981.

Shi, X. F., Shen, S. X., Yi, H.-I., Chen, Z. H., and Meng, Y.: Modern sedimentary environments and dynamic depositional systems in the southern Yellow Sea, Chin. Sci. Bull., 48, 1–7, https://doi.org/10.1007/BF02900933, 2003.

Shinn, Y. J., Chough, S. K., Kim, J. W., and Woo, J.: Development of depositional systems in the southeastern Yellow Sea during the postglacial transgression, Mar. Geol., 239, 59–82, https://doi.org/10.1016/j.margeo.2006.12.007, 2007.

Song, Y.-H. and Choi, M. S.: REE geochemistry of fine-grained sediments from major rivers around the Yellow Sea. Chem. Geol., 266, 328–342, https://doi.org/10.1016/j.chemgeo.2009.06.019, 2009.

Sukigara, C., Mino, Y., Tripathy, S. C., Ishizaka, J., and Matsuno, T.: Impacts of the Changjiang diluted water on sinking processes of particulate organic matters in the East China Sea, Cont. Shelf Res., 151, 84–93, https://doi.org/10.1016/j.csr.2017.10.012, 2017.

Taylor, S. R. and McLennan, S. M.: The Continental Crust: Its Composition and Evolution, Blackwell, Oxford, 312 pp, 1985.

Uehara, K. and Saito, Y.: Late Quaternary evolution of the Yellow/East China Sea tidal regime and its impacts on sediment dispersal and seafloor morphology, Sediment. Geol., 162, 25–38, https://doi.org/10.1016/S0037-0738(03)00234-3, 2003.

Wang, L., Sarnthein, M., Erlenkeuser, H., Grimalt, J., Grootes, P., Heilig, S., Ivanova, E., Kienast, M., Pelejero, C., and Pflaumann, U.: East Asian monsoon climate during the Late Pleistocene: high-resolution sediment records from the South China Sea, Mar. Geol., 156, 245–284, https://doi.org/10.1016/S0025-3227(98)00182-0, 1999.

Wang. L., Yang, Z., Zhang, R. P., Fan, D. J., Zhao, M. X., and Hu, B. Q.: Sea surface temperature records of core ZY2 from the central mud area in the South Yellow Sea during last 6200 years and related effect of the Yellow Sea Warm Current, Chin. Sci. Bull., 56, 1588–1595, https://doi.org/10.1007/s11434-011-4442-y, 2011.

Wang, F., Liu, C., and Meng, Q.: Effect of the Yellow Sea warm current fronts on the westward shift of the Yellow Sea warm tongue in winter, Cont. Shelf Res., 45, 98–107, https://doi.org/10.1016/j.csr.2012.06.005, 2012.

Wang, Q. and Yang, S. Y.: Clay mineralogy indicates the Holocene monsoon climate in the Changjiang (Yangtze River) Catchment, China, Appl. Clay Sci., 74, 28–36, https://doi.org/10.1016/j.clay.2012.08.011, 2013.

Wang, Y., Li, G., Zhang, W., and Dong, P.: Sedimentary environment and formation mechanism of the mud deposit in the central South Yellow Sea during the past 40 kyr, Mar. Geol., 347, 123–135, https://doi.org/10.1016/j.margeo.2013.11.008, 2014.

Wei, J. W., Shi, X. F., Li, G. X., and Liang, R. C.: Clay mineral distributions in the southern Yellow Sea and their significance, Chin. Sci. Bull., 48, 7–11, https://doi.org/10.1007/BF02900934, 2003.

Xiang, R., Yang, Z. S., Saito, Y., Fan, D. J., Chen, M. H., Guo, Z. G., and Chen, Z.: Paleoenvironmental changes during the last 8400 years in the southern Yellow Sea: Benthic foraminiferal and stable isotopic evidence, Mar. Micropaleontol., 67, 104–119, https://doi.org/10.1016/j.marmicro.2007.11.002, 2008.

Xu, D., Liu, X., Zhang, X., Li, T., and Chen, B.: China Offshore Geology,. Geological Publishing House, Beijing, 310 pp, 1997.

Xu, Z. K., Lim, D. I., Choi, J. Y., Yang, S. Y., and Jung, H. J.: Rare earth elements in bottom sediments of major rivers around the Yellow Sea: implications for sediment provenance, Geo.-Mar. Lett., 29, 291–300, https://doi.org/10.1007/s00367-009-0142-x, 2009.

Xu, Z. K., Li, T. G., Chang, F. M., Wan, S. M., Choi, J. Y., and Lim, D. I.: Clay-sized sediment provenance change in the northern Okinawa Trough since 22 kyr BP and its paleoenvironmental implication, Palaeogeogr. Palaeoclimatol. Palaeoecol., 399, 236–245, https://doi.org/10.1016/j.palaeo.2014.01.016, 2014.

Yang, Y. S., Jung, H. S., Choi, M. S., and Li, C. X.: The rare earth element compositions of the Changjiang (Yangtze) and Huanghe (Yellow) river sediments, Earth Planet. Sci. Lett., 201, 407–419, https://doi.org/10.1016/S0012-821X(02)00715-X, 2002.

Yang, S. Y., Jung, H. S., Lim, D. I., and Li, C. X.: A review on the provenance discrimination of sediments in the Yellow Sea. Earth-Sci. Rev., 63, 93–120, https://doi.org/10.1016/S0012-8252(03)00033-3, 2003.

Yang, Z. S. and Liu, J. P.: A unique Yellow River-derived distal subaqueous delta in the Yellow Sea. Mar. Geol., 240, 169–176, https://doi.org/10.1016/j.margeo.2007.02.008, 2007.

Yang, S. Y. and Youn, J.-S.: Geochemical compositions and provenance discrimination of the central south Yellow Sea sediments. Mar. Geol., 243, 229–241, https://doi.org/10.1016/j.margeo.2007.05.001, 2007.

Yoo, D. G., Koo, N.-H., Lee, H.-Y., Kim, B.-Y., Kim, Y.-J., and Cheong, S.: Acquisition, processing and interpretation of high-resolution seismic data using a small-scale multi-channel system: an example from the Korea Strait inner shelf, south-east Korea, Explor. Geophys., 47, 341–351, https://doi.org/10.1071/EG15081, 2015.

Yoo, D.-G., Lee, G.-S., Kim, G.-Y., Kang, N.-K., Yi, B.-Y., Kim, Y.-J., Chun, J.-H., and Kong, G.-S.: Seismic stratigraphy and depositional history of late Quaternary deposits in a tide-dominated setting: An example from the eastern Yellow Sea, Mar. Pet. Geol., 73, 212–227, https://doi.org/10.1016/j.marpetgeo.2016.03.005, 2016.

Zhao, Y. Y., Qin, Z. Y., Li, F. Y., and Chen, Y. W.: On the source and genesis of the mud in the central area of the south Yellow Sea, Chin. J. Oceanol. Limnol., 8, 66–73, https://doi.org/10.1007/BF02846453, 1990.

Zhang, W., Xing, Y., Yu, L., Feng, H., and Lu, M.: Distinguishing sediments from the Yangtze and Yellow Rivers, China: a mineral magnetic approach, Holocene, 18, 1139–1145, https://doi.org/10.1177/0959683608095582, 2008.